

Pockel's effect and optical rectification in (111)-cut near-intrinsic silicon crystals

Zhanguo Chen,¹ Jianxun Zhao,¹ Yuhong Zhang,² Gang Jia,^{1,a)} Xiuhuan Liu,³ Ce Ren,¹ Wenqing Wu,¹ Jianbo Sun,¹ Kun Cao,¹ Shuang Wang,¹ and Bao Shi¹

¹State Key Laboratory on Integrated Optoelectronics, College of Electronic Science and Engineering, Jilin University, 2699 Qianjin Street, Changchun 130012, People's Republic of China

²Jilin Architectural and Civil Engineering Institute, Changchun 130021, People's Republic of China

³College of Communication Engineering, Jilin University, 2699 Qianjin Street, Changchun 130012, People's Republic of China

(Received 16 April 2008; accepted 1 June 2008; published online 26 June 2008)

Pockel's effect and optical rectification are demonstrated in the charge space region of a (111)-cut near-intrinsic silicon crystal by the use of a planar metal-insulator-semiconductor structure. The results show that both Pockel's effect and optical rectification are so considerable that these effects should be taken into account for designing silicon-based photonic devices. The anisotropy of optical rectification is measured too, and experimental results are in good accordance with the theoretical analysis. These effects can also be used as a tool to investigate the properties of the charge space region of silicon devices in future. © 2008 American Institute of Physics.
[DOI: 10.1063/1.2952462]

As the most important semiconductor material, most microelectronic devices are based on silicon. Since silicon is transparent for the 1.3 and 1.55 μm fiber-optic communication wavelengths, silicon photonics is also developing as an intriguing subject.^{1–3} All kinds of silicon-based photonic devices, such as silicon-based Raman laser,^{4,5} silicon-on-insulator waveguides,^{6,7} Mach-Zehnder interferometer modulators,^{8,9} and silicon-based microdisk resonators,^{10,11} have been manufactured. Although silicon is a centrosymmetric material and the second-order nonlinear susceptibility $\chi^{(2)}$ is zero in the bulk according to the dipole approximation, it exhibits a considerable second-order dipole response at the surface because the inversion symmetry is broken.¹² Electric field is also able to break the inversion symmetry¹³ and produce the so-called electric-field-induced second-order nonlinear optical effect, such as second-harmonic generation (SHG).^{14–16} The electric-field-induced SHG has been used as a powerful tool for investigating the properties of the surface and interface of silicon microelectronics.^{17–20}

Optical rectification (OR) and Pockel's effect (PE) also belong to the second-order nonlinear optical effects, however, we have not found any reports about these effects in silicon devices. In fact, these effects might play an important role in silicon photonics since PE can change the polarization state of light and OR can induce a polarized field in silicon. In this letter, PE and OR in the space charge region (SCR) of silicon crystal at the wavelength of 1.342 μm is demonstrated. Compared to the free carrier plasma dispersion effect,⁹ PE is stronger in our experiment. As the reverse effect of PE, OR is measured too. The anisotropy of OR is investigated.

The (111) surface of silicon possesses C_{3v} symmetry.¹² Since there exists the built-in dc electric field in SCR, the inversion symmetry of silicon crystal can also be broken in SCR. The SCR under the (111) surface of silicon also exhibits C_{3v} symmetry.²¹ That means that the SCR under the (111) surface of silicon can be taken as a uniaxial crystal whose

optical axis is [111] axis. So the second-order nonlinear optical effects, such as SHG, PE, and OR, should exist in SCR. According to the theory of PE,²² if a modulating electric field $E = E_0 \cos(\Omega t)$ is applied along the [111] axis, and the probing beam propagates along the [11 $\bar{2}$] direction, then, the phase retardation can be written as

$$\Delta\phi = \Delta\phi_0 + \Delta\phi(E), \quad (1a)$$

$$\Delta\phi_0 = 2\pi l(n_e - n_o)/\lambda, \quad (1b)$$

$$\Delta\phi(E) = \pi l(n_e^3\gamma_{33} - n_o^3\gamma_{13})E/\lambda, \quad (1c)$$

where n_e and n_o are refractive indices of the extraordinary light and the ordinary light, respectively, l is the propagating length, λ is the wavelength of probing beam in vacuum, and γ_{33} and γ_{13} are electro-optic coefficients in SCR of silicon. $\Delta\phi_0$ is the natural phase retardation because of the surface symmetry and subsurface SCR, and $\Delta\phi(E)$ is the phase retardation due to PE.

In order to study PE in silicon, we construct a transverse electro-optic amplitude modulator, shown in Fig. 1. The sample is a planar metal-insulator-semiconductor (MIS) capacitor structure, shown in Fig. 1(a). For removing charge-carrier effects,²³ a near-intrinsic (111)-cut silicon crystal is used as the sample, whose resistivity is around 4000 Ωcm .

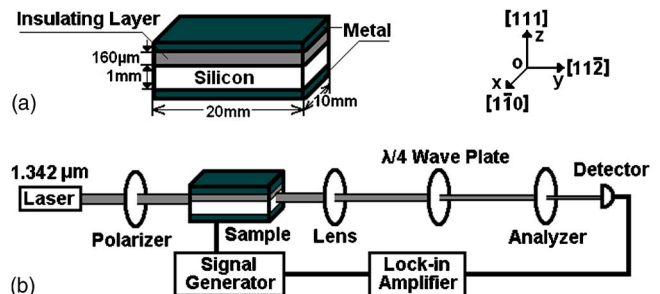


FIG. 1. (Color online) Configuration of silicon sample and the measuring system for PE. (a) MIS configuration of silicon sample, whose size and orientation are denoted. (b) Experimental setup for PE measurements.

^{a)}Electronic mail: jiagang@jlu.edu.cn.

So the carrier density is about $1.2 \times 10^{12} \text{ cm}^{-3}$. The size of silicon sample is $1 \times 10 \times 20 \text{ mm}^3$. Side surfaces are the $(1\bar{1}0)$ and $(11\bar{2})$ planes, and the $(11\bar{2})$ planes are polished to diminish the energy loss when the light passing through. The work functions of the metal electrode and the semiconductor are different, if the insulator is thin, electrons will transfer between the metal and the semiconductor, and the Fermi levels become the same finally. In order to eliminate this effect, and keep the original state of silicon surface, a thick enough ($160 \mu\text{m}$) polyester insulating layer was filled between the metal electrode and silicon sample. The total electric capacity of the sample structure without bias, about 33 pF , is measured. The dielectric constant of the insulating layer is 3.0 and the electric capacity of the insulating layer C_i is about 33.2 pF . According to the carrier density, the Debye length L_D at the silicon surface can be calculated as

$$L_D = \sqrt{\epsilon_0 \epsilon_{rs} kT / Ne^2}, \quad (2)$$

where ϵ_0 is the permittivity of free space, $\epsilon_{rs} = 12$ is the dielectric constant of silicon, k is the Boltzmann constant, T is the absolute temperature in kelvins, N is the carrier density, and e is the elementary charge. The result is $L_D \approx 3.8 \mu\text{m}$ at 300 K . Thus, we estimate the flat band capacity of silicon is about 5.6 nF with the small signal model. Even if in the inversion mode of operation, the capacity of SCR is not less than 1.2 nF yet. So most applied voltage will drop on the insulating layer, and only a little voltage will drop on the subsurface SCR of silicon sample, and the small signal modulating model will be satisfied.

The structure of the electro-optic amplitude modulator is a modification of the Senarmont compensator,²⁴ shown in Fig. 1(b). The $[111]$ axis of silicon, namely, z axis, is vertical in the space. The polarization of the analyzer is parallel to the z axis, while the polarizer and the fast axis of the quarter wave plate is 45° with respect to the z axis. Calculated by the Jones matrix, the intensity of the output beam I_o can be obtained

$$I_o = I_i [1 \pm \sin(\Delta\phi)]/2 \approx I_i [1 \pm \Delta\phi(E)]/2, \quad (3)$$

where I_i is the intensity of the input beam and $\Delta\phi$ is the phase retardation generated when the beam passing through the sample, which is small and defined as Eqs. (1a)–(1c). As for silicon SCR, $n_e \approx n_o$, so $\Delta\phi_0$ is very small and can almost be ignored. Otherwise, we just need to adjust the analyzer slightly to ensure Eq. (3).

In experiments, a 200 mW cw laser operating at the wavelength of $1.342 \mu\text{m}$ is used as the light source, and a 770 Hz sine signal from the signal generator is biased on the sample. The output beam is somewhat dispersed when coming out from silicon, so a long-focus lens is used for focusing it on a Ge photodetector, and the electro-optic signal is measured by a lock-in amplifier. From Eqs. (1a)–(1c) and (3), the relationship between the measured electro-optic signal V_{eo} and the applied voltage V_{appl} can be written as

$$V_{eo} = \frac{1}{2} \alpha I_{in} \frac{\pi}{V_\pi} \frac{C_i}{C_i + C_s} V_{appl}, \quad (4)$$

where $V_\pi = \lambda d / (n_e^3 \gamma_{33} - n_o^3 \gamma_{13}) l$ is the half-wave voltage, α is the factor depending on the photodetector and lock-in amplifier, d is the effective charge layer thickness, and C_s is the effective capacity of silicon sample.

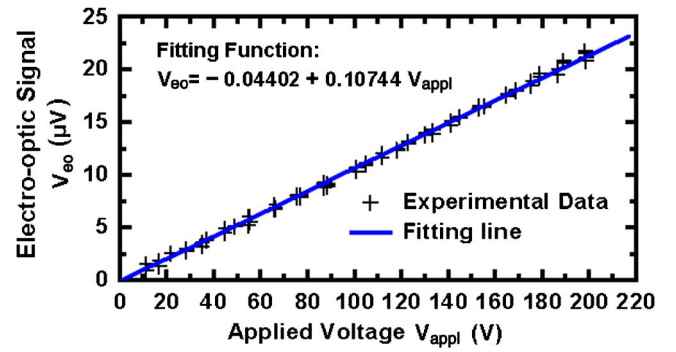


FIG. 2. (Color online) Dependence of electro-optic signals on the applied voltage. The electro-optic response is linear for the applied voltage changed from 10 up to 200 V .

The measured electro-optic response curve is shown in Fig. 2. This is a very good linear response for the applied voltage changed from 10 up to 200 V . In fact, the real modulating voltage drop on the SCR of silicon with the depth of the Debye length is only from 60 mV to 1.2 V or so at the modes of accumulation or flatband. In order to obtain the half-wave voltage V_π , we remove the signal generator and insert a chopper into the measuring system shown in Fig. 1(b). Thus, the optical signal is measured and it is about 25 mV . The input beam is not focused lest the multiphoton absorption takes effect.²⁵ The waist of the input beam is about 1 mm , but only the light passing through the SCR (about $4.0 \mu\text{m}$ thickness) can contribute to the electro-optic signal, so the practical light signal in Eq. (4) is much less than 25 mV . Assume that $\alpha I_{in}/2 \approx 1 \text{ mV}$, according to the slope of the response line shown in Fig. 2, we estimate the half-wave voltage V_π is at most about 170 V .

It is well known that modulation of the refractive index in silicon can also be achieved via the free carrier plasma dispersion effect.²³ According to the relative theory,⁹ the half-wave voltage contributed by the plasma dispersion effect can be expressed as

$$V'_\pi = 5.68 \times 10^{26} e d_i d / \epsilon_0 \epsilon_{rs} l, \quad (5)$$

where d_i is the thickness of insulating layer, d is the effective charge layer thickness, and all variables and constants are in international units. Assume that $d = 1 \mu\text{m}$ (the same magnitude as L_D), we can obtain $V'_\pi = 9.2 \times 10^3 \text{ V}$. Since $V'_\pi \gg V_\pi$, the free carrier plasma dispersion effect can be ignored in our experiments. That is, the measured electro-optic signal is mainly contributed by PE in SCR of the silicon.

OR can be taken as the inverse effect of PE. They should exist simultaneously in the SCR of silicon sample. A simple OR measuring system is designed, shown in Fig. 3. The orientation of silicon sample is the same as that in Fig. 2. If the azimuth of the linear polarized light is θ with respect to the

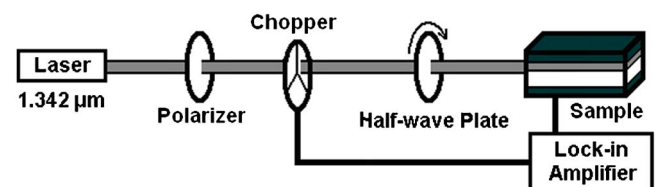


FIG. 3. (Color online) Experimental setup for OR measurements. A half-wave plate is used for changing the azimuth of the linear polarization light.

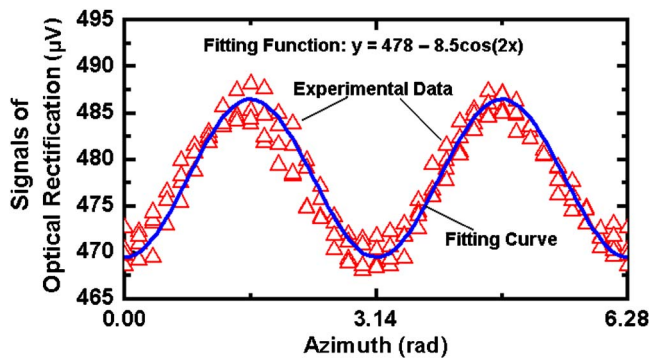


FIG. 4. (Color online) The measured anisotropy of OR at the (111) surface of silicon crystal. The solid line is the fitting curve according to a cosine function with a period π , which is in good accordance with the experimental data and the theory.

x axis (namely, $[1\bar{1}0]$ axis), then the dc polarization along the z axis can be expressed as

$$P_z^0 = \varepsilon_0 E_0^2 \{ [\chi_{zzz}^{(2)} + \chi_{zxx}^{(2)}] - [\chi_{zzz}^{(2)} - \chi_{zxx}^{(2)}] \cos(2\theta) \}, \quad (6)$$

where E_0 is the electric-field intensity of the probing beam and $\chi_{zzz}^{(2)}$ and $\chi_{zxx}^{(2)}$ are effective second-order susceptibilities in the SCR of silicon. Thus, a z axis dc polarization field will be generated when a cw laser beam passes through the silicon SCR. When a chopper is inserted into the light pass, an ac polarization voltage signal generated from the metal electrodes of silicon sample can be detected by a lock-in amplifier. By rotating the half-wave plate to change the azimuth of the linear polarized light, we measured the anisotropy of OR, shown in Fig. 4, which is in good accordance with Eq. (6). However, in Fig. 4, note that the measured voltage signal has a considerable background which is independent of the azimuth θ . Possible causes are analyzed. (i) The values of $\chi_{zzz}^{(2)}$ and $\chi_{zxx}^{(2)}$ are very close, therefore, the term independent of the azimuth θ is much larger than the one dependent of θ in Eq. (6). If other reasons are neglected, according to the fitting function in Fig. 4, the ratio of $\chi_{zxx}^{(2)}/\chi_{zzz}^{(2)} \approx 0.965$ can be achieved. (ii) Due to the residual linear absorption associated with defects, impurities, and surfaces,²⁶ some photocarriers are generated near the surface and separated by surface electric field. At ac condition, photocarriers will be collected by the electrodes, which may produce a detectable voltage signal independent of the azimuth θ . (iii) Two-photon absorption (TPA) can also produce photocarriers,^{27,28} which might also contribute to the measured voltage signal. However, we do not focus the input beam, so TPA should be weak. According to the anisotropy of TPA, in our experiments, the effective third-order nonlinear susceptibility dependent of the azimuth θ should be expressed as²⁹

$$\chi_{\text{eff}}^{(3)}(\theta) = \chi_{xxxx}^{(3)} \left[1 - \frac{2}{3} \sigma \left(\frac{3}{4} \sin^4 \theta + \cos^4 \theta \right) \right], \quad (7)$$

in which, $\sigma = [\chi_{xxxx}^{(3)} - (\chi_{xyxy}^{(3)} + 2\chi_{xyyx}^{(3)})] / \chi_{xxxx}^{(3)}$. Nevertheless, the experimental data cannot match Eq. (7), so TPA and other multiphoton absorption processes can be ignored in OR experiments. (iv) Due to SHG in silicon SCR, double frequency absorption (DFA) may also affect the measured signal.³⁰ In our experiments, the phase matching condition is not be considered, and the probing beam is not be focused, so SHG should be feeble, and DFA can be neglected too.

In summary, we observed PE and OR in the SCR of a (111)-cut near-intrinsic silicon crystal. These effects take

place because the inversion symmetry is broken in silicon SCR by the dc electric field. As for near-intrinsic silicon, the depth of SCR is typically several microns, so these effects can be taken as bulk effects, and they are very considerable. In our experiments, PE is much stronger than the free carrier plasma dispersion effect. So these effects must be considered in designing the silicon-based photonic devices, such as optical waveguides, and optical modulators. Moreover, at the interfaces, such as the p - n junction, or other SCRs of silicon devices, these effects should also be detectable, so they may also be used as a tool to study the properties of surfaces and interfaces of silicon devices.

This work was supported by the National Natural Science Foundation of China, (Program Nos. 60506016 and 60476027), and Collaborative projects of NSFC-RFBR agreement (Program No. 60711120182).

- ¹B. Jalali and S. Fathpour, *J. Lightwave Technol.* **24**, 4600 (2006).
- ²M. Salib, L. Liao, R. Jones, M. Morse, A. Liu, D. Samara-Rubio, D. Alduino, and M. Paniccia, *Intel Technol. J.* **8**, 143 (2004).
- ³R. A. Soref, S. J. Emelett, and W. R. Buchwald, *J. Opt. A, Pure Appl. Opt.* **8**, 840 (2006).
- ⁴O. Boyraz and B. Jalali, *Opt. Express* **12**, 5269 (2004).
- ⁵H. Rong, R. Jones, A. Liu, O. Cohen, D. Hak, A. Fang, and M. Paniccia, *Nature (London)* **433**, 725 (2005).
- ⁶P. D. Trinh, S. Yegnanarayanan, F. Coppinger, and B. Jalali, *IEEE Photonics Technol. Lett.* **9**, 940 (1997).
- ⁷A. Liu, H. Rong, and M. Paniccia, *Opt. Express* **12**, 4261 (2004).
- ⁸L. Liao, D. Samara-Rubio, M. Morse, A. Liu, and D. Hodge, *Opt. Express* **13**, 3129 (2005).
- ⁹A. Liu, R. Jones, L. Liao, D. Samara-Rubio, D. Rubin, O. Cohen, R. Nicolaescu, and M. Paniccia, *Nature (London)* **427**, 615 (2004).
- ¹⁰P. Koonath, T. Indukuri, and B. Jalalib, *Appl. Phys. Lett.* **86**, 091102 (2005).
- ¹¹K. J. Vahala, *Nature (London)* **424**, 839 (2003).
- ¹²J. E. Sipe, D. J. Moss, and H. M. van Driel, *Phys. Rev. B* **35**, 1129 (1987).
- ¹³J. Qi, M. S. Yeganeh, I. Koltover, A. G. Yodh, and W. M. Theis, *Phys. Rev. Lett.* **71**, 633 (1993).
- ¹⁴G. Lüpke, C. Meyer, C. Ohlhoff, H. Kurz, S. Lehmann, and G. Marowsky, *Opt. Lett.* **20**, 1997 (1995).
- ¹⁵A. Bouhelier, M. Beversluis, A. Hartschuh, and L. Novotny, *Phys. Rev. Lett.* **90**, 013903 (2003).
- ¹⁶O. A. Aktsipetrov, A. A. Fedyanin, A. V. Melnikov, E. D. Mishina, and A. N. Rubtsov, *Phys. Rev. B* **60**, 8924 (1999).
- ¹⁷D. Xiao, E. Ramsay, D. T. Reid, B. Offenbeck, and N. Weber, *Appl. Phys. Lett.* **88**, 114107 (2006).
- ¹⁸C. Ohlhoff, C. Meyer, G. Lüpke, T. Löffler, T. Pfeifer, H. G. Roskos, and H. Kurz, *Appl. Phys. Lett.* **68**, 1699 (1996).
- ¹⁹T. V. Dolgova, A. A. Fedyanin, and O. A. Aktsipetrov, *Phys. Rev. B* **68**, 073307 (2003).
- ²⁰G. Lüpke, C. Meyer, C. Ohlhoff, H. Kurz, S. Lehmann, and G. Marowsky, *Opt. Lett.* **20**, 1997 (1995).
- ²¹O. A. Aktsipetrov, A. A. Fedyanin, V. N. Golovkina, and T. V. Murzina, *Opt. Lett.* **19**, 1450 (1994).
- ²²A. Yariv, *Introduction to Optical Electronics* (Holt, Rinehart and Winston, New York, 1976).
- ²³R. A. Soref and B. R. Bennett, *IEEE J. Quantum Electron.* **23**, 123 (1987).
- ²⁴Y. Lu, Z.-Y. Cheng, S. Park, S.-F. Liu, and Q. Zhang, *Jpn. J. Appl. Phys., Part 1* **39**, 141 (2000).
- ²⁵J. Zhang, Q. Lin, G. Piredda, R. W. Boyd, G. P. Agrawal, and P. M. Fauchet, *Appl. Phys. Lett.* **91**, 071113 (2007).
- ²⁶M. Hass and B. Bendow, *Appl. Opt.* **16**, 2882 (1977).
- ²⁷T. K. Liang, H. K. Tsang, I. E. Day, J. Drake, A. P. Knights, and M. Asghari, *Appl. Phys. Lett.* **81**, 1323 (2002).
- ²⁸L. P. Barry, P. G. Bollond, J. M. Dudley, J. D. Harvey, and R. Leonhardt, *Electron. Lett.* **32**, 1922 (1996).
- ²⁹R. DeSalvo, M. Sheik-Bahae, A. A. Said, D. J. Hagan, and E. W. Van Stryland, *Opt. Lett.* **18**, 194 (1993).
- ³⁰X. Liu, B. Shi, G. Jia, Z. Chen, C. Ren, Y. Zhang, K. Cao, and J. Zhao, *Appl. Phys. Lett.* **90**, 101109 (2007).